Eta Model Storm-Relative Winds Associated with Tornadic and Nontornadic Supercells

RICHARD L. THOMPSON

NOAA/NWS Storm Prediction Center, Norman, Oklahoma

(Manuscript received 18 December 1996, in final form 9 September 1997)

ABSTRACT

A conceptual model for sustained low-level mesocyclones is tested as a tornado forecast tool with observations and forecasts from the operational Eta Model. In the conceptual model, a balance between low-level storm inflow and outflow allows the development of a persistent low-level mesocyclone along the rear flank of a supercell thunderstorm, owing largely to the strength of the midlevel storm-relative winds. The present work draws on this conceptual model to identify preferred ranges of low- (model surface level), middle- (500 mb), and upper-level (250-mb) storm-relative wind speeds for 131 supercells, from gridded Eta Model fields. The observations reveal that the 500-mb storm-relative wind speed has a distinct lower bound of approximately 8 m s^{-1} for the tornadic supercells, while differences between surface-level and 250-mb storm-relative wind speeds for tornadic and nontornadic supercells are much less pronounced. The storm-relative wind speeds are also compared to the bulk Richardson number shear for the purpose of discriminating between tornadic and nontornadic supercells. Test results of storm-relative wind speed at the Eta Model surface level and at 500 mb, derived from gridded Eta forecast fields, demonstrate skill in distinguishing tornadic and nontornadic supercells in daily forecast operations at the Storm Prediction Center.

1. Introduction

Prediction of tornadoes has presented a great challenge to meteorologists since the inception of modern severe thunderstorm forecasting. Pioneering efforts of the Air Weather Service in the late 1940s and early 1950s led to a methodology of forecasting tornadoes (e.g., Fawbush et al. 1951) based on a checklist of parameters to diagnose atmospheric stability and wind structure, much of which remains in use today. Later work in the 1950s focused on so-called proximity soundings to reveal thermodynamic characteristics of the tornadic thunderstorm environment (Fawbush and Miller 1952, 1954; Beebe 1958), such as the Miller type-I ''loaded gun'' sounding (not shown). These studies led to analyses of vertical wind profiles in proximity to tornadic thunderstorms (e.g., Darkow 1969; Darkow and Fowler 1971), as well as to understanding the characteristics of environmental storm-relative winds associated with tornadic and nontornadic severe thunderstorms (Maddox 1976).

Severe thunderstorm research conducted during recent years has refined our understanding of the relationships between supercell thunderstorms (those with persistent mesocyclones) and the ambient vertical wind shear. Theoretical studies (Davies-Jones 1984; Lilly 1986) have demonstrated the relationship between low-level (approximately 0–2 or 0–3 km above ground level) storm-relative helicity (hereafter SRH) and midlevel (approximately 3–6 km above ground level) mesocyclones in supercell thunderstorms. Other theoretical studies (e.g., Rotunno and Klemp 1985) and numerical modeling (e.g., Weisman and Klemp 1982, 1984) have revealed the link between supercells and vertical shear from the low to midlevels. SRH has been used routinely as a tornado forecast tool (Davies-Jones et al. 1990) since the early 1990s, though SRH more accurately identifies *supercell* environments (Brooks et al. 1993). A combination of convective available potential energy (CAPE) and SRH has also served as a tornado forecast tool (Johns et al. 1993), via the energy–helicity index [EHI; Hart and Korotky (1991); Davies (1993)]. The bulk Richardson number (BRN, Weisman and Klemp 1982) shear has also been used effectively to identify supercell environments (e.g., Weisman and Klemp 1982, 1984, 1986; Droegemeier et al. 1993, hereafter DLD93; Jahn and Droegemeier 1996). More recently, the shear term from the BRN has been applied to numerical mesoscale model forecasts with the goal of discriminating between tornadic and nontornadic thunderstorm environments (Weisman and Klemp 1982; Stensrud et al. 1997, hereafter SCB97). In the BRN denominator, as calculated by SCB97, U_{avg} is defined as the magnitude of the difference between the 0–6-km density-weighted mean wind and the density-weighted mean wind in the lowest 0.5 km:

Corresponding author address: Richard L. Thompson, NOAA/NWS Storm Prediction Center, 1313 Halley Circle, Norman, OK 73069.
E-mail: richard.thompson@noaa.gov

$$\text{BRN shear} = 0.5(u_{\text{avg}})^2.$$

Numerical simulations of supercells have begun to elucidate processes relevant to supercell tornadogenesis, and the Verification of the Origins of Rotation in Tornadoes Experiment (VORTEX; Rasmussen et al. 1994) has provided detailed measurements near and within tornadic supercells. Significant contributions to understanding tornadogenesis have been presented by Klemp and Rotunno (1983), Rotunno and Klemp (1985), Klemp (1987), Wicker and Wilhelmson (1995), and Wicker (1996), among others. These studies emphasize the characteristics of the environmental and storm-induced wind shear profiles, especially at low levels (e.g., 0–500 m above ground level). Specifically, low-level vertical wind shear along the forward flank baroclinic zone of a supercell, as well as generation of horizontal baroclinic vorticity, have been linked to the strength of the low-level mesocyclone. Detailed, high-resolution observations and forecasts of low-level vertical wind profiles would be necessary to test these conceptual models in forecast operations, but such data are generally unavailable to operational meteorologists. The present study focuses on another conceptual model for sustained low-level mesocyclones with tornadic supercells proposed by Davies-Jones and Brooks (1993). This conceptual model focuses on the importance of the storm-relative midlevel winds to create a balance between low-level storm inflow (DLD93) and low-level outflow near the rear flank of a supercell thunderstorm. The strength of the low-level outflow along the rear flank of a supercell is modulated by the tendency for precipitation to advect downwind from the mesocyclone or become wrapped around the storm updraft. At one extreme, weak storm-relative winds in the midlevels allow a large amount of precipitation to wrap around the mesocyclone within a supercell thunderstorm, leading to the generation of excessive rain-cooled outflow along the rear flank of the supercell. This rain-cooled air often ''undercuts'' the midlevel mesocyclone and disrupts the low-level mesocyclone and the production of long-lived or multiple supercell tornadoes. At the other extreme, excessive storm-relative wind speeds in the midlevels remove too much precipitation downwind from the midlevel mesocyclone, which inhibits the development of rain-cooled outflow along the rear flank of a supercell. This rain-cooled downdraft along the rear flank of the storm is associated with baroclinic vorticity generation and *may* ultimately serve as a source for vertical vorticity near the ground for the low-level mesocyclone. Therefore, low-level vorticity production is limited if little rain-cooled outflow is present along the rear flank of a supercell. Between these extremes a balance can exist between the production of vertical vorticity in the downdraft along the rear flank and the tendency for this downdraft to undercut the supercell in the low levels. It is implied by Davies-Jones and Brooks (1993) that supercells producing multiple and/or long-lived tornadoes fall in this middle range where the rear flank downdraft is pronounced and balanced by storm inflow. Such a supercell structure appears to favor the repeated production of tornadoes.

The present work follows that of Davies-Jones and Brooks (1993), Brooks et al. (1994a, hereafter BDW94) and Brooks et al. (1994b, hereafter BDC94). Consideration of storm inflow and middle-/upper-level storm-relative wind speeds appears to provide a more complete picture of the environment favoring supercells with sustained *low-level* mesocyclones and tornadoes than do BRN, SRH, or EHI, which are more specifically associated with *midlevel* mesocyclones. A methodology of documenting analyses and testing forecasts of storm-relative wind speeds in the low, middle, and upper levels is developed using output from the Eta Model (Black 1994) over the conterminous United States. Results of the 22-month period of study are presented with a discussion of applicability to operational forecasting of tornadic supercells.

2. Data and methodology

The 80-km horizontal resolution ''early'' Eta Model run was chosen to test the storm-relative conceptual model for tornadic supercells. These forecast data are widely available to National Weather Service field offices through the Personal Computer-based Gridded Interactive Display and Diagnostic System (PCGRIDDS; Zubrick and Thaler 1993). The horizontal resolution of the Eta Model changed to 48 km in October 1995, although the PCGRIDDS display resolution remained unchanged. Eighty-one of the 131 supercell cases occurred after the Eta Model resolution change, but this resolution change in the Eta Model did not have a noticeable impact on the PCGRIDDS diagnoses or forecasts of storm-relative wind speed. Eta Model storm-relative (hereafter SR) wind speeds were evaluated for both tornadic and nontornadic supercells; SR wind speeds were calculated from Eta Model initial hour PCGRIDDS data based on observed supercell motions. Given the many problems associated with choosing proximity soundings (see BDC94) and with data availability, the Eta initial hour analyses were used in lieu of soundings to diagnose SR wind speeds. Based on the results of this diagnostic assessment of supercells from 1995 and 1996, Eta Model forecasts of SR wind speeds were evaluated for a subset of supercell cases from 1995. Eta Model forecast data were not available for many of the 1996 cases, thus limiting the forecast evaluation to 1995 cases.

The low-, middle-, and upper-level SR wind speeds were defined in terms of available terrain following surfaces or pressure levels in PCGRIDDS. Low-level inflow was set at the Eta Model surface level (located 15 mb ''above'' the model ground, hereafter referred to as the surface level), while midlevel relative wind speed was calculated at 500 mb. These are crude approximations to 0–2-km inflow (DLD93) and 2–9-km relative

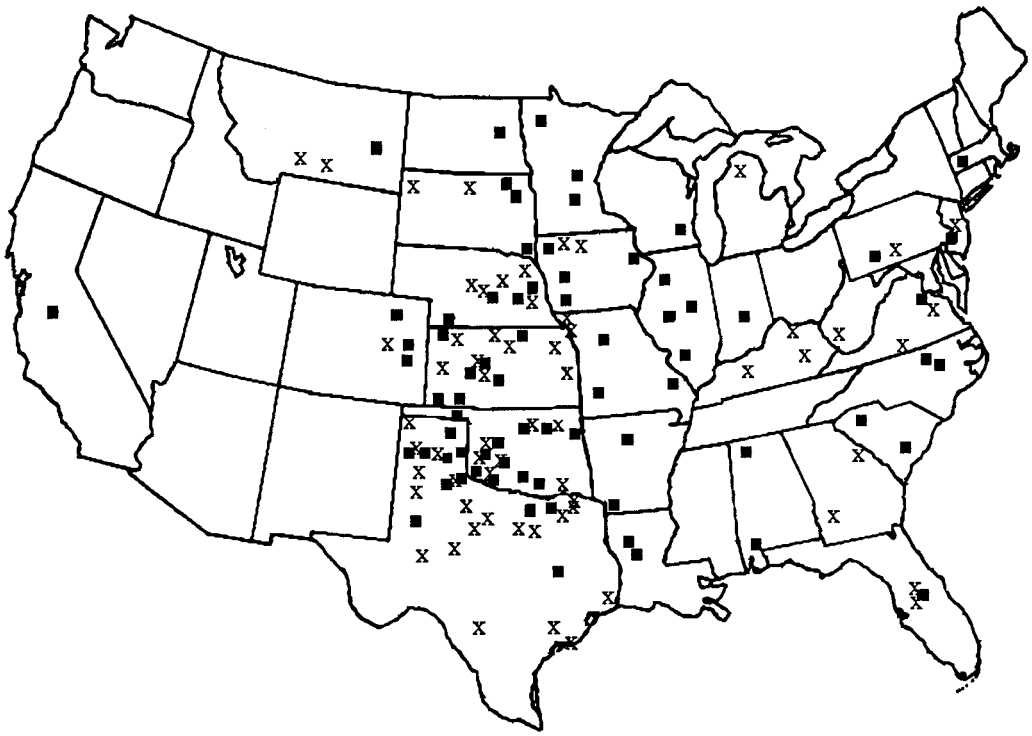

FIG. 1. Geographic plot of approximate model gridpoint locations for supercells in this study. Solid squares denote supercells with multiple or long-lived tornado reports, and each × represents a nontornadic supercell.

flow (BDC94), limited by the coarse vertical resolution of the Eta Model PCGRIDDS data. The anvil-level relative wind speed (Rasmussen and Straka 1998, hereafter RS) was calculated at 250 mb. Anvil-level relative flow may be important to precipitation efficiency and rainfall distribution in supercells. Storm-relative winds near the anvil may largely determine whether developing precipitation particles form and fall out near the main storm updraft or are advected downwind in the anvil (RS). Additionally, the BRN shear was modified to fit the PCGRIDDS data. The 0–6- and 0–0.5-km density-weighted mean winds of the BRN shear were replaced with the Eta surface-level to 400-mb density-weighted mean wind and the surface-level wind, respectively.

Tornadic and nontornadic supercell cases were collected for the 22-month period beginning in November 1994 and ending in August 1996. To be considered, the following criteria must have been met.

1) To be called a supercell, a ''storm'' must have displayed Weather Surveillance Radar-1988 Doppler (WSR-88D) reflectivity (e.g., hook echo and weak echo region) and velocity signatures (WSR-88D mesocyclone algorithm) associated with supercells (after Browning 1964; Lemon 1977; Doswell and Burgess 1993). Radar data were augmented by *Storm Data* descriptions, and video or eyewitness reports when available.
2) The supercell must have occurred within 3 h of an Eta Model initialization (i.e., between 0900 and 1500 or 2100 and 0300 UTC).
3) PCGRIDDS data were available for the Eta Model initialization.

Actual storm motion was calculated from radar reflectivity mosaics by tracking the reflectivity centroid for 1 h, centered on the times of tornado report(s) or the most pronounced radar signatures if nontornadic. This storm motion was then used to calculate the storm-relative wind speed for the surface level, 500 mb, and 250 mb with the initial hour Eta Model winds for the closest grid point to the supercell.

Locations of model grid points associated with 131 supercell cases are depicted in Fig. 1. A majority of the supercells occurred across the central and southern Great Plains, with the greatest concentration near the Texas–Oklahoma border. The prevalence of southern plains supercells in this database represents the tendency for plains supercells to occur during the data collection time in this study (viz., 2100–0300 UTC). Some supercells over the high plains developed too late in the evening to be considered, and a few supercells east of the Mississippi River dissipated prior to 2100 UTC. Only four supercells in this study occurred during the morning time period (0900–1500 UTC). Not surprisingly, the majority of the southern plains supercells occurred from April to June, while most of the supercells from Colorado to Minnesota occurred during June and

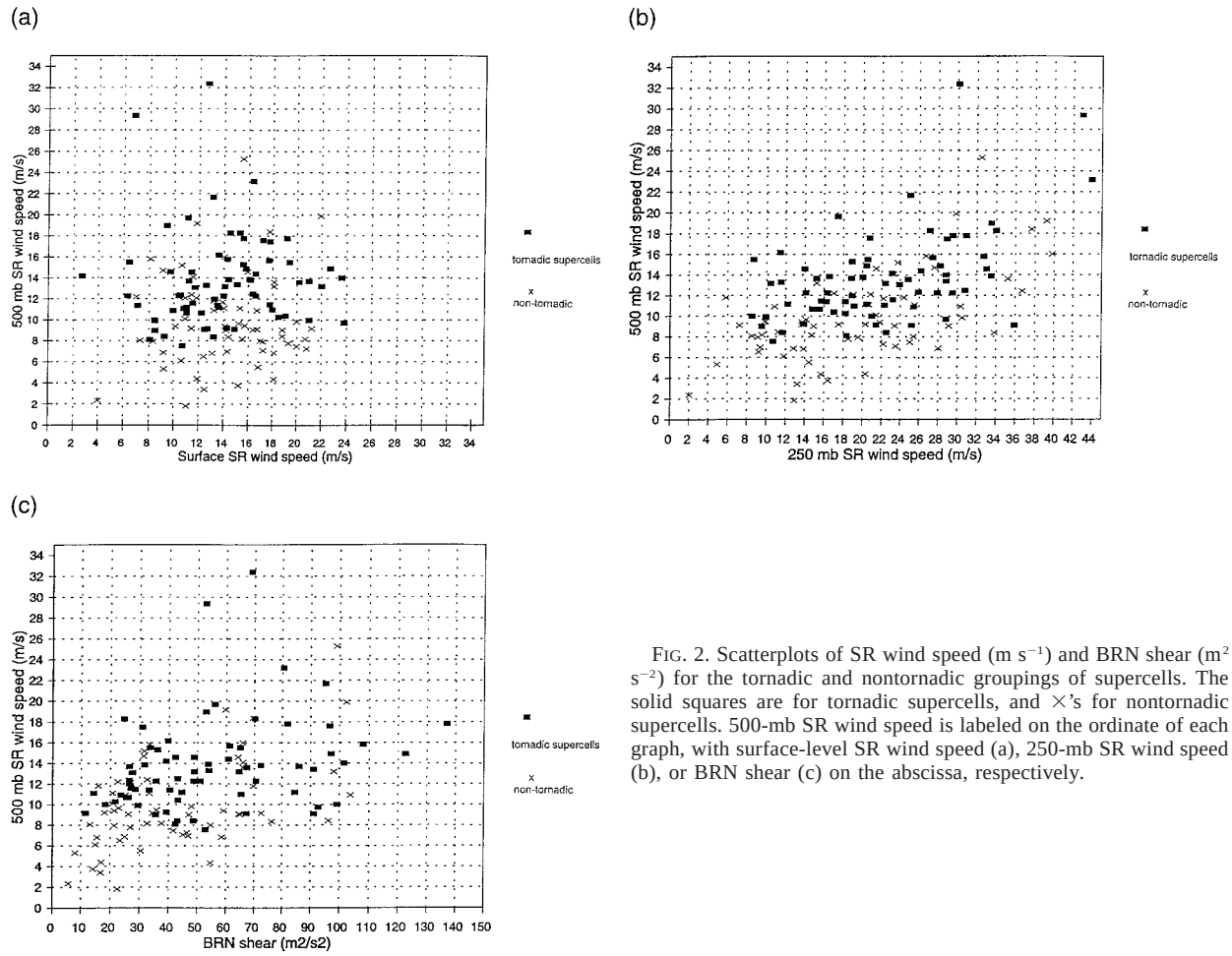

FIG. 2. Scatterplots of SR wind speed (m s^{-1}) and BRN shear (m^2 s^{-2}) for the tornadic and nontornadic groupings of supercells. The solid squares are for tornadic supercells, and ×'s for nontornadic supercells. 500-mb SR wind speed is labeled on the ordinate of each graph, with surface-level SR wind speed (a), 250-mb SR wind speed (b), or BRN shear (c) on the abscissa, respectively.

July. The supercells affecting the gulf coast and southeast Atlantic coast areas occurred during the cool season from late October to mid-April.

Storm Data was the preferred source for tornado reports, although *Storm Data* was not yet available for the 1996 cases. Thus, the Storm Prediction Center Rough Log of severe weather reports became a substitute. Several difficulties were encountered in distinguishing between tornadic and nontornadic supercells, as well as supercell and nonsupercell tornadoes. The latter were addressed by assuming tornadoes were supercellular only if a storm was identified as a supercell 15 min *prior* to the first tornado report with the storm. This check does not guarantee a particular tornado was indeed supercellular. However, this criterion reduces the chance of falsely identifying a nonsupercell tornado as supercellular, namely when radar signatures similar to a supercell evolve simultaneously with a nonsupercell tornado (Wakimoto and Wilson 1989). Also, a supercell cannot be classified as nontornadic with complete certainty. Darkness, remote areas, and a lack of damage can all preclude a tornado from being reported. Doswell and Burgess (1988) discuss many issues related to the quality of tornado reports in *Storm Data.*

Twenty of the supercells in this study produced a single tornado, with the tornadoes described as being ''brief'' or as producing no damage. Classifying supercells as tornadic based on such reports seemed an inadequate means of testing a conceptual model for *sustained* low-level mesocyclones. To more clearly infer the influence of SR wind speed in sustaining low-level mesocyclones and associated tornadoes, supercells were classified as tornadic when the indication was unambiguous. For this study, a supercell was designated tornadic on the basis of multiple tornado reports and/or the occurrence of a long-lived (>15 min) tornado. Supercells with only a single brief/weak tornado were included in the nontornadic category since the conceptual model does not preclude a brief tornado *without* a long-lived mesocyclone in the low levels.

3. Results of SR flow diagnostic evaluation

The SR wind magnitudes were calculated for the surface level, 500 mb, and 250 mb for the tornadic and

TABLE 1. Summary of mean values and standard deviations (STD) of the surface-level (SFC), 500- and 250-mb SR wind speeds (m s^{-1}), and BRN shear (m^2 s^{-2}) for the three groupings of supercells. Values in parentheses indicate the number of supercells in each group.

	Tornadic (69)		Nontornadic (62)	
	Mean (m s^{-1})	STD (m s^{-1})	Mean (m s^{-1})	STD (m s^{-1})
SFC	13.9	4.4	14.2	3.9
500 mb	13.7	4.4	9.9	4.3
250 mb	22.1	8.0	19.8	8.9
BRN shear	54.8 m^2 s^{-2}	27.7 m^2 s^{-2}	42.1 m^2 s^{-2}	25.0 m^2 s^{-2}

nontornadic supercells. Scatter diagrams of the SR wind speeds and BRN shear are presented in Figs. 2a–c.

a. Surface-level and 500-mb SR wind speeds

The surface-level SR wind speed plots are similar for the tornadic and nontornadic supercells, but important differences stand out at 500 mb. Figure 2a shows a similar clustering of nontornadic values to that of the tornadic supercells at the surface, with substantial overlap between the two groups at 500 mb. The range of surface-level SR wind speeds is very similar for both the tornadic and nontornadic storms, with mean values near 14 m s^{-1} for each group. However, the mean values of 500-mb SR wind speed are 13.7 m s^{-1} for the tornadic cases, and 9.9 m s^{-1} for the nontornadic supercells, as depicted in Table 1. The standard deviations of the 500-mb SR wind speeds for the tornadic and nontornadic supercells are 4.4 and 4.3 m s^{-1}, respectively. Considering the difference in the means of 3.8 m s^{-1} between the tornadic and nontornadic supercells and the standard deviations near 4.4 m s^{-1}, one might consider the differences between the two samples to be statistically significant. Indeed, a *t* test reveals that the difference in the means is statistically significant at the 99% confidence level.

A categorization of SR wind speeds with the tornadic and nontornadic supercells is shown in Table 2. It is noteworthy that 61% (38 of 62) of the nontornadic supercells were associated with 500-mb SR wind speeds less than 10 m s^{-1}, while 81% (56 of 69) of the tornadic supercells were associated with greater than 10 m s^{-1} 500-mb SR wind speeds. Also, 87% (60 of 69) of the tornadic cases are clustered in the range from 8 to 19 m s^{-1}. Figure 2a displays a clear lower bound to the 500-mb SR wind magnitude for the tornadic cases, with all but one of the 69 cases exhibiting 500-mb SR wind speeds greater than 8 m s^{-1}. A lower bound to SR surface level wind speed is not as apparent as with the 500-mb SR wind speeds, though most of the values range from 8 to 22 m s^{-1}. The mean low- and midlevel SR wind speeds with the tornadic supercells agree favorably with the 0–1-km (~surface level) and 5–6-km (~500 mb) SR mean speeds for F2 or greater tornado proximity soundings from Kerr and Darkow (1996), as well as with the estimated storm-relative winds at the surface and 500 mb from Maddox (1976; see Maddox's Figs. 8, 9, and 11).

The analysis suggests that 500-mb SR wind speed best differentiates between the tornadic and nontornadic supercells in this study. It is also important to note that while all of the tornadic supercells were associated with 500-mb SR wind speed of 7.9 m s^{-1} or greater, several of the nontornadic storms also had comparable midlevel SR wind speeds to the tornadic cases. This suggests 500-mb SR wind speed of 8 m s^{-1} or greater is a necessary, but not sufficient, condition for tornadic supercells (refer to Fig. 2a).

b. SR wind speeds at 250 mb

The 250-mb SR wind speeds cover a similar range of values for both the nontornadic and tornadic supercells (Fig. 2b). At 250 mb, SR wind magnitudes are well distributed between a lower bound around 8 m s^{-1} and an apparent upper bound near 35 m s^{-1} (Fig. 2b). The apparent upper bound to the 250-mb SR wind speed may be meaningful in terms of its effect on precipitation efficiency and rainfall distribution in a supercell (RS). However, the upper bound in this sample may simply reflect the approximate climatological maximum 250-mb wind speed in which supercells occur in the United States. The large range of 250-mb SR wind speeds does imply that a wide variation of supercell structures can support the development of tornadoes, from ''heavy precipitation'' supercells (Doswell et al. 1990b) associated with weak anvil-level relative winds, to ''low precipitation'' supercells (Bluestein and Parks 1983) associated with strong anvil-level relative wind speeds. In the case of the heavy-precipitation supercell, precipitation particles form and fall out near the main updraft of the

TABLE 2. Categorical distributions of SR wind speed for the surface level (SFC), 500 mb, 250 mb, and BRN shear for the tornadic and nontornadic supercells. Numeric values represent percentage of total cases in each group within each category.

	Tornadic (69)				Nontornadic (62)			
	<10 m s^{-1}	10–25 m s^{-1}	>25 m s^{-1}	>35 m s^{-1}	<10 m s^{-1}	10–25 m s^{-1}	>25 m s^{-1}	>35 m s^{-1}
SFC	0.19	0.81	—	—	0.13	0.87	—	—
500 mb	0.16	0.81	0.03	—	0.61	0.37	0.02	—
250 mb	0.06	0.56	0.38	0.03	0.16	0.57	0.27	0.03
	<25 m^2 s^{-2}	25–100 m^2 s^{-2}	>100 m^2 s^{-2}		<25 m^2 s^{-2}	25–100 m^2 s^{-2}	>100 m^2 s^{-2}	
BRN shear	0.09	0.85	0.06		0.32	0.65	0.03	

supercell due to weak anvil-level relative winds. The author speculates that the opposite can occur with some supercells tending toward the low-precipitation end of the spectrum where strong anvil-level relative winds remove developing precipitation particles downwind from the main updraft, much as speculated by Branick and Doswell (1992) concerning the 13 March 1990 supercell tornado outbreak.

c. BRN shear versus 500-mb SR wind speed

A comparison of 500-mb SR wind speeds to the BRN shear for the tornadic and nontornadic supercells is displayed in Fig. 2c. The BRN shear displays an approximate lower bound for the tornadic supercells near 25 $m^2 s^{-2}$, and only 6% of the values are greater than 100 $m^2 s^{-2}$. This range of BRN shear values from 25 to 100 $m^2 s^{-2}$ is in general agreement with the range of values proposed by SCB97 for tornadic storms. BRN shear magnitudes for the nontornadic supercells were generally less than with the tornadic supercells, with a clustering of values from about 20–50 $m^2 s^{-2}$ (Fig. 2c). The lower BRN shear values reflect the weaker environmental wind shear associated with the nontornadic supercells, but a relatively large percentage (39%) of nontornadic cases still exceed the lower bound of 40 $m^2 s^{-2}$ used by SCB97 to forecast tornadic supercells.

Care must be given in interpreting differences in the BRN shear values from different numerical models [e.g., Eta vs the fourth-generation Pennsylvania State University–NCAR Mesoscale Model (MM4) used by SCB97]. The BRN shear term is sensitive to low-level winds and, in turn, sensitive to the boundary layer parameterization. Also, the vertical resolution of the Eta PCGRIDDS data available for this study is coarser than the MM4 model and can introduce errors in BRN shear calculations. One might expect a general increase in 500-mb SR wind speed with increasing BRN shear since BRN shear depends largely on midlevel wind speed. However, the stronger vertical wind shear associated with larger BRN shear values often contributes to a faster storm motion; thus, the relationship between BRN shear and 500-mb SR wind speed is not necessarily straightforward. Figure 2c shows only a slight tendency for SR wind speed at 500 mb to increase as BRN shear increases (linear correlation coefficient of 0.30 for the tornadic supercells and 0.44 for combined tornadic and nontornadic). Therefore, caution is advised when using the methodology of SCB97 where BRN shear serves as a surrogate for midlevel SR wind speed. However, 500-mb SR wind speeds (for this dataset) are generally 8 m s^{-1} or greater for BRN shear values greater than 25 $m^2 s^{-2}$; thus, BRN shear may also have value as a supercell tornado forecast parameter.

4. Prognostic evaluation of the storm-relative conceptual model

Two basic forecast parameters were evaluated with the Eta Model PCGRIDDS data using vector differences with an estimated storm motion: SR wind speed at the model surface level and SR wind speed at 500 mb. The parameters of surface-level and 500-mb SR wind speed were combined with an arbitrary CAPE threshold of 500 J kg^{-1} in PCGRIDDS to delineate areas favorable for supercells with sustained low-level mesocylones and associated tornadoes. Using the location of the closest grid point to each tornadic and ''nontornadic'' supercell, SR wind speeds were calculated for the 24- and 12-h forecasts valid at the time of the initial hour analysis (0000 UTC in 127 of 131 cases).

The lower limits of favorable surface-level and 500-mb SR wind speed for tornadic supercells were defined as 8 m s^{-1} based on results of the diagnostic evaluation (section 3). Though surface-level SR wind speed does not appear to discriminate between tornadic and nontornadic supercells, the lower bound near 8 m s^{-1} is still important for supercells in general (see scatterplots and Tables 1 and 2). Gridpoint forecast errors were also compiled for the tornadic and nontornadic samples. Errors were based on comparisons between the 24- and 12-h forecasts with the verifying SR wind speeds derived from Eta 0-h analyses and observed storm motions. Additionally, initial hour ''forecast errors'' were calculated by taking the difference between initial hour Eta SR wind speeds based on an *assumed* deviant storm motion and SR speeds using the *observed* storm motions.

An estimated storm motion is necessary when examining forecasts of SR wind speeds and processes related to supercell tornadogenesis, and an assumed deviant motion is relevant since this SR technique *assumes the presence of a supercell.* Forecasting supercells is a somewhat different problem than identifying the potential for *tornadic* supercells, and a detailed discussion on some problems with forecasting supercells based on storm-relative shear parameters can be found in Weisman (1996). To determine storm motion a priori, a motion of 30° right and 75% of the 1000–500-mb mean wind speed is assumed (after Maddox 1976). For the high plains (defined as west of 100°W longitude), the Eta Model 1000-mb and 850-mb winds are basically the same, so storm motion estimates for this region were based on the 850–400-mb mean wind. This assumed motion of the supercells can be in error when the wind profile does not lie in the upper-right quadrant of the hodograph, as discussed by Weisman and Klemp (1986) and Weisman (1996). For example, Weisman and Klemp (1986) present various wind profiles and associated storm motions (refer to their Fig. 15.16). In part b of the figure (with a wind profile in the lower portions of the hodograph), the rightward supercell motion is actually *faster* than the mean wind, similar to a left moving (anticyclonic) supercell with a wind profile in the upper-right portion of the hodograph.

5. Results of SR flow forecast test

Forecast data were collected and analyzed for January–December of 1995. The diagnostic assessment led

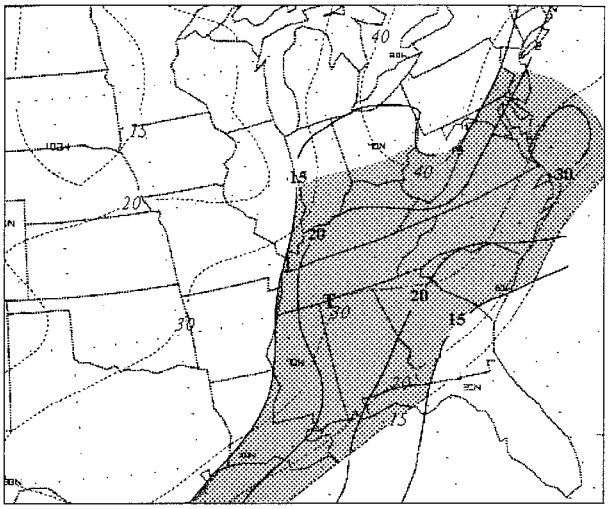

FIG. 3. Eta Model 12-h forecast valid 0000 UTC 19 May 1995. Solid contours (with bold labels) are SR wind speed (kt) at the surface level, and dashed contours (with italic labels) are SR wind speed at 500 mb. Only the 15-, 20-, 30-, and 40-kt SR wind speed contours are displayed for both the surface and 500 mb. The stippled area is the overlap of 15-kt (~8 m s^{-1}) SR wind speeds at the surface and 500 mb, only in the region of CAPE greater than 500 J kg^{-1}. The approximate location of the tornadic supercell(s) used in the diagnostic assessment is marked by a T.

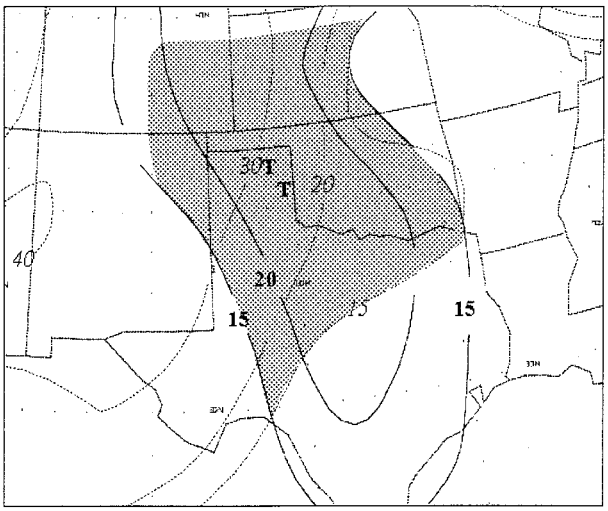

FIG. 4. Eta 12-h forecast valid 0000 UTC 8 June 1995. Conventions are the same as in Fig. 3.

to the proposed SR wind speed guidelines for tornadic supercells, namely, the lower bounds to surface-level and 500-mb SR wind speed of 8 m s^{-1}. Figure 3 is an example of the forecast output with 8 m s^{-1} (~15 kt) lower bounds valid at 0000 UTC 19 May 1995, and data are displayed in knots for consistency with observed and forecast data available to National Weather Service meteorologists. A significant tornado outbreak was in progress from Kentucky to northern Alabama at the valid time of this forecast. The supercell used in this study produced violent (F4 damage) tornadoes in northern Alabama, in an area of nearly 15 m s^{-1} (~30 kt) forecast surface and 500-mb SR wind speeds. The SR wind speeds associated with this storm are well within the distribution of values associated with tornadic supercells (refer to Fig. 2a). Another case of long-lived, violent tornadoes (F4 damage) occurred across the eastern Texas panhandle during the afternoon and evening hours of 8 June 1995, and the 12-h SR wind speed forecast valid at 0000 UTC 9 June 1995 is depicted in Fig. 4. These tornadic supercells were well within the forecast overlap area of SR wind speeds and CAPE. Both cases also met the criteria for tornadic supercells in 0-h analyses using the assumed and observed storm motions (not shown). On a note of caution, the 8 June 1995 case illustrates a more general problem with the verification of forecasts of rare events. Prior to the violent tornado-producing storms, a nontornadic supercell existed well within the forecast tornadic region. This SR forecast technique appears to be best suited to forecasting the ''worst'' event in a region, where tornadic storms are worse than nontornadic storms, but does not ensure *all* storms in a region will be tornadic.

The 21 July 1995 and 23 July 1995 cases (Figs. 5 and 6, respectively) are forecasts for less ''synoptically evident'' (see Johns and Doswell 1992) events than the two previous examples. During the evening hours of 21 July 1995, several supercells produced 14 tornadoes (8 resulted in F1–F2 damage) in the vicinity of Minneapolis, Minnesota. The large-scale pattern consisted of 15–20 m s^{-1} (~30–40 kt) westerly 500-mb flow and weak (5–7 m s^{-1}) surface to 850-mb flow from the southwest over Minnesota at 1200 UTC 21 July 1995, and observed CAPE (lifting the ''most unstable parcel'' in the lowest 70 mb) less than 100 J kg^{-1}. The Eta Model run that morning forecast destabilization during the day over Minnesota, as well as an increase in low-

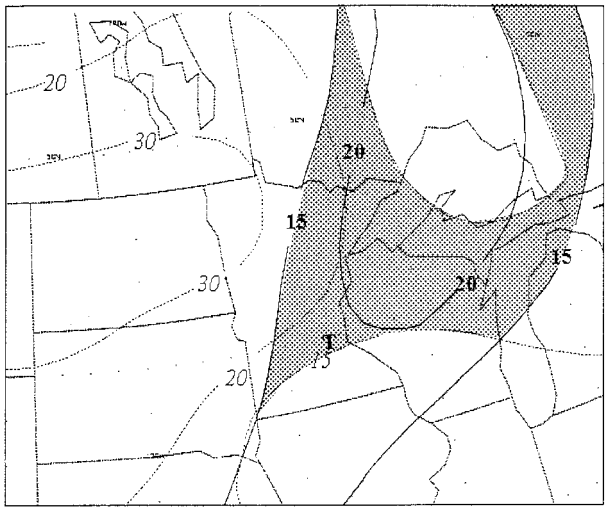

FIG. 5. Eta 12-h forecast valid 0000 UTC 21 July 1995. Conventions are the same as in Fig. 3.

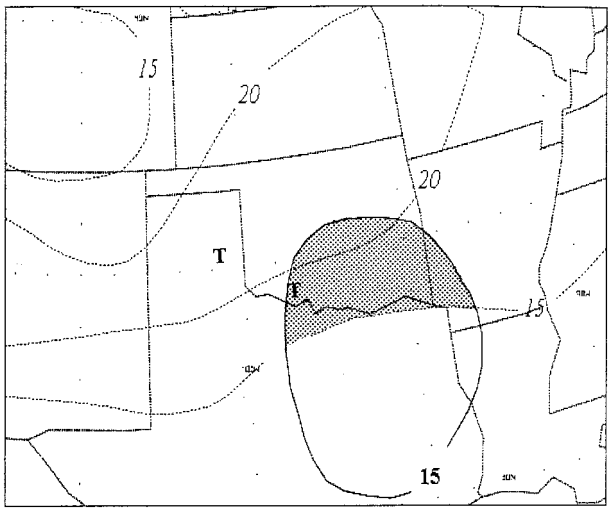

FIG. 6. Eta 12-h forecast valid 0000 UTC 24 July 1995. Conventions are the same as in Fig. 3.

level wind speeds to about 10 m s^{-1} (~20 kt). Though the described conditions are not normally considered ''synoptically evident'' for supercell tornadoes, SR wind speed forecasts from the Eta Model more clearly identified potential for tornadoes (see Fig. 5), assuming supercells developed.

An example of a subtle supercell tornado forecast case (23 July 1995) is given in Fig. 6, which consisted of several tornadic supercells near a convective outflow boundary from the eastern Texas panhandle to the southwest corner of Oklahoma. The 12-h forecast shows sufficient inflow for sustained tornadic supercells over parts of southern and southwest Oklahoma, but not as far northwest as the eastern Texas panhandle (Fig. 6). However, wind profiles from Frederick, Oklahoma, and Amarillo, Texas (not shown), indicated greater than 12 m s^{-1} (~25 kt) surface SR wind speeds over the eastern Texas panhandle, along and immediately north of an outflow boundary left by convection the previous night. The mesoscale nature of the outflow boundary may explain why the larger-scale Eta Model analyses were unable to provide sufficient detail to diagnose the influence of this boundary on low-level SR winds.

Forecast statistics were computed for 51 of the 1995 supercell cases (28 tornadic, 23 nontornadic) included in the diagnostic assessment, based on availability of 24- and 12-h PCGRIDDS forecast data for the initial hour analysis time. The forecast was for tornadic supercells (as described in section 2) when surface-level and 500-mb SR wind speeds were forecast to be greater than 8 m s^{-1} in the 24- and 12-h forecasts at the location of the observed supercell. Forecasts were considered nontornadic when at least one of the surface-level or 500-mb SR wind speeds remained <8 m s^{-1} for either the 12- or 24-h forecast. Verifying observations were classified as either ''tornadic'' (multiple and/or long-lived tornadoes) or ''nontornadic'' (includes supercells with a single brief/weak tornado). Results of this forecast test are presented in a contingency table (Table 3, after Doswell et al. 1990a).

TABLE 3. Contingency table for the combined 24- and 12-h Eta Model wind speed forecasts for the 1995 supercells used in the diagnostic assessment: Y represents tornadic supercells, N represents nontornadic supercells, POD is the probability of detection, FAR is the false alarm ratio, and CSI is the critical success index.

		Observed			
		Y	N	Sum	
Forecast	Y	24	13	37	POD 0.86
	N	4	10	14	FAR 0.35
	Sum	28	23	51	CSI 0.59

The 8 m s^{-1} thresholds resulted in a probability of detection for tornadic supercells of 85% (24 of 28) in the present study. The false alarm ratio for the 1995 forecast test was 35% (13 of 37), which combines with the 85% probability of detection to yield a 0.59 critical success index. More sophisticated measures of forecast skill, such as the true skill statistic and Heidke score [both near 0.30 for this forecast test; see Doswell et al. (1990a)] applied to rare event forecasting, take into account correct forecasts that arise purely by chance. The verification in this study differs from Doswell et al. (1990a) in that numerous correct forecasts of no tornadic supercells are *not* included (since the SR technique is only relevant when supercells occur), thus the Heidke score and true skill score are quite similar.

Forecast error statistics

Error statistics were compiled for the 1995 forecast cases included in the diagnostic evaluation. Storm-relative wind speed and CAPE (most unstable parcel in lowest 70 mb) forecasts for the subset of 51 supercells (28 tornadic, 23 nontornadic) from 1995 were calculated at the same grid points used in the diagnostic evaluation. Storm-relative wind speeds, based on the initial hour Eta wind analyses and observed storm motions, and CAPE were subtracted from 24-, 12-, and initial hour forecasts based on the assumed storm motion 30° to the right and 75% of the 1000–500-mb mean wind (850–400-mb mean wind for the high plains region). In addition, magnitude (i.e., percent of 1000–500-mb mean speed) and direction errors were calculated at each supercell grid point by comparing the assumed motion with the observed storm motion.

Error statistics are summarized in Table 4. Storm-relative wind speed forecasts at 500 mb displayed only small negative biases for the entire group of tornadic and nontornadic supercells, with mean errors near -2.0 m s^{-1}. The entire forecast dataset shows no significant bias for surface-level SR wind speed. A few biases become more apparent when considering tornadic and nontornadic cases separately. For the tornadic supercells, surface-level SR wind speed was on average ov-

TABLE 4. Mean and mean absolute (abs) gridpoint forecast errors of SR wind speed for the 51 supercell cases (ALL) from 1995, as well as separate groupings of tornadic (TORN) and nontornadic (NON) supercells. Observed SR wind speeds are subtracted from the initial hour, 12-, and 24-h forecasts (F00, F12, F24) valid within 3 h of each supercell, where positive values are overforecasts (too strong) and negative values are underforecasts (too weak). The SR wind speed errors for the surface level (SFC), 500, and 250 mb are in m s^{-1}, and CAPE forecast errors are in J kg^{-1}. Total numbers of supercells in each grouping are in parentheses.

	F00			F12			F24		
	(51) ALL	(28) TORN	(23) NON	ALL	TORN	NON	ALL	TORN	NON
SFC	−0.3	1.4	−2.3	−0.1	1.5	−2.0	0.2	1.5	−1.4
Abs	3.4	3.4	3.4	4.4	4.9	3.6	4.4	5.1	3.4
500	−1.0	−1.7	−0.1	−2.6	−3.0	−2.1	−1.7	−3.1	−0.1
Abs	2.8	2.9	2.6	3.6	3.8	3.3	4.2	3.0	3.6
250	−0.2	−1.1	0.9	0.6	0.4	0.8	−0.4	0.1	−0.9
Abs	2.8	2.8	2.7	5.3	4.6	6.3	5.9	5.9	6.0
CAPE				27	−63	136	−10	−176	193
Abs				484	548	405	640	735	524

erforecast by 1–2 m s^{-1}, while it was underforecast by roughly the same degree for the nontornadic storms. Opposite biases were noted at 500 mb, with a slight tendency to underforecast SR speed in the tornadic cases, and no clear bias with the nontornadic cases. Overall, no significant bias was noted in forecasts of 250 mb SR wind speed. Finally, forecasts of CAPE displayed noteworthy biases in that CAPE was overforecast by almost 200 J kg^{-1} at 24 h for the nontornadic storms and underforecast by almost 200 J kg^{-1} for the tornadic storms. This bias in CAPE forecasts should be an important consideration when applying SR wind speed forecasts. Specifically, Eta Model forecasts during the period of this study had a tendency to underforecast CAPE in association with tornadic supercells, which typically led to an underestimate of the northern and eastern extent of the supercell tornado threat area during cool season events. Additionally, 12-h CAPE forecasts were less than 1500 J kg^{-1} for 55% of the tornadic supercells and 45% of the nontornadic supercells from the 1995 subset. Such modest forecast CAPE values could lead the unwary forecaster to underestimate the threat of supercells in the first place.

Standard deviations of forecast errors ranged from near 4 m s^{-1} at the surface and 500 mb to 8–9 m s^{-1} at 250 mb. Absolute error distributions for the 24-, 12-, and 0-h forecasts are presented in Fig. 7. These standard deviations are large compared to the mean errors, owing to errors of opposite sign tending to cancel one another. Mean absolute errors are somewhat larger

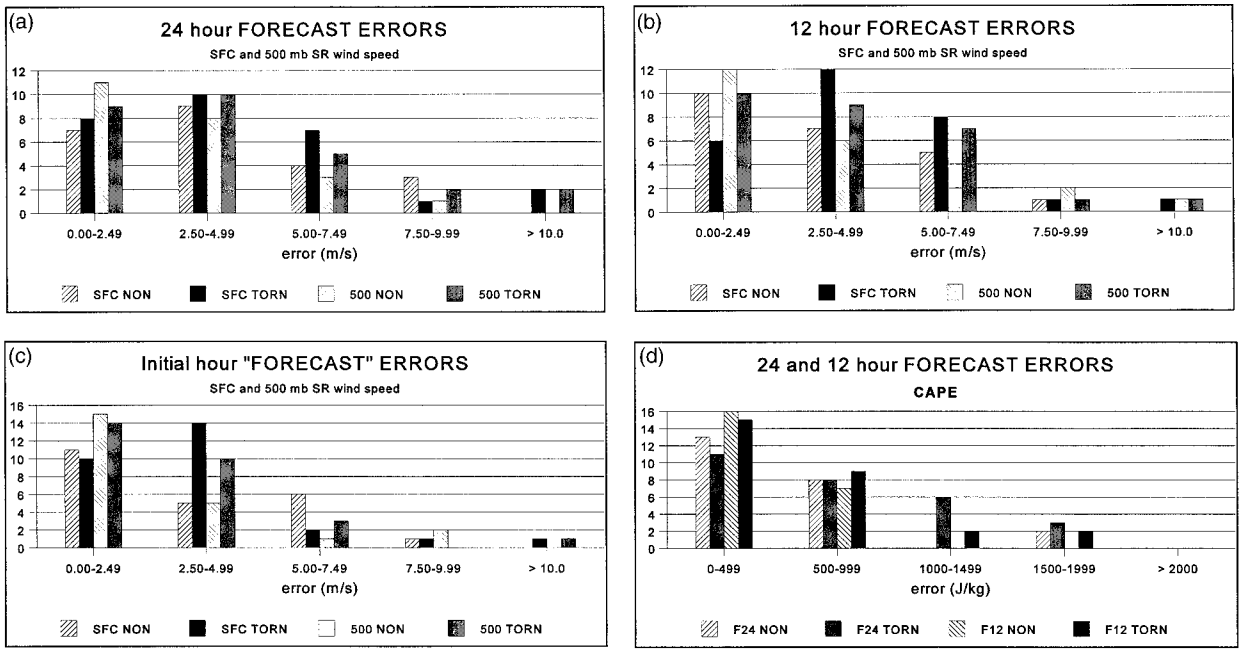

FIG. 7. Categorical distributions of absolute SR wind speed forecast errors for the surface level and 500 mb for the (a) 24-h forecast, (b) 12-h forecast, and (c) initial hour ''forecast'' (based on assumed motion). CAPE forecast errors at 24 and 12 h are displayed in (d).

than the mean errors, with values ranging from 3.5 to 5.0 m s^{-1} at the surface and 500 mb for the 12- and 24-h forecasts. The standard deviations and mean absolute errors for the surface-level and 500-mb SR wind speed forecasts are large enough to warrant concern when applying the Eta SR wind speed forecasts to supercell tornado forecasting. The standard deviation of about 4 m s^{-1} in forecast errors at 500 mb is comparable to the difference in the mean between the 500-mb SR wind speeds for the tornadic and nontornadic supercells. Operational forecasters must be wary of such forecast errors and pay particular attention to model forecast trends.

Magnitude and direction errors revealed several biases inherent to the assumed storm motion in this study. The tornadic supercells closely matched the assumed motion, with a mean deviation of 31° to the right and a speed 82% of the 1000–500-mb mean wind. However, the mean nontornadic supercell motion was faster (119% of the 1000–500-mb mean speed) and more to the right (37°). The faster and more deviant rightward motion of the nontornadic storms explains the tendency to underestimate surface-level SR wind speed. It appears the Eta Model tended to underforecast 500-mb wind speeds, which supports the tendency of 500-mb SR wind speeds to be underforecast for the tornadic supercells. Though no significant bias was noted in 500-mb SR wind speed forecasts for the nontornadic supercells, it appears likely that the observed faster storm motions were generally offset by stronger than forecast 500-mb wind speeds.

6. Discussion

Of the three SR parameters examined, the 500-mb SR wind speed distinguished the tornadic supercells most successfully. A sharp lower bound to the 500-mb SR wind speed is apparent in Fig. 2a ($\sim$8 m s^{-1}), with a less defined upper bound near 19 m s^{-1}. The apparent upper bound to the 500-mb SR wind speed *may* represent a general upper limit for sustained supercells, but the number of cases in the upper range of SR wind speed is too small to clearly confirm or refute this possibility. Storm-relative wind speeds at the surface and 250 mb span very similar ranges of values for both the tornadic and nontornadic supercells, respectively. The 250-mb SR wind speed does exhibit a lower cutoff near 8 m s^{-1} and an apparent upper limit near 35 m s^{-1} for the tornadic cases (Fig. 2b), while the SR surface-level wind speeds range primarily from 8 to 22 m s^{-1} for the tornadic cases. Very little difference is apparent between the mean values and ranges of surface-level SR wind speed for the tornadic and nontornadic cases, unlike the 500-mb SR wind speed where mean values for the tornadic storms are nearly 4 m s^{-1} greater than the nontornadic supercells. These data suggests the 500-mb SR wind speed is the most effective mandatory-level SR parameter (of those tested) in distinguishing between tornadic and nontornadic supercells.

Colquhoun and Riley (1996) found the surface to 600-mb shear magnitude to be the parameter best correlated to tornado ''intensity'' (F-scale damage rating) in their tornado proximity sounding database. Similar to the BRN shear, the surface to 600-mb shear is even more heavily influenced by midlevel wind speeds.

It is important to note that substantial overlap exists between the SR wind speeds for the tornadic and nontornadic supercells. The 500-mb SR wind speeds for many of the nontornadic supercells fall well within the cluster of SR wind speeds associated with the tornadic supercells, meaning the SR conceptual model does not guarantee a supercell will produce tornadoes. On the other hand, weak 500-mb SR wind speed ($<$8 m s^{-1}) seems to preclude all but a brief and/or weak tornado with a supercell.

The surface-level SR wind speed was relatively weak ($<$10 m s^{-1}) for about 20% of the tornadic supercells (refer to Fig. 2a and Table 2). Possible explanations for this weakness include poor Eta analyses or mesoscale features noted in surface data that could have enhanced storm inflow. For example, at least three supercells produced several F4 tornadoes in western Iowa during the evening of 27 May 1995. The Eta analysis of surface-level SR wind speed (not shown) yielded values less than 7 m s^{-1} for these storms, while substitution of actual surface observations resulted in inflow greater than 10 m s^{-1}. In addition, nearby profilers and the velocity azimuth display wind profiles from the WSR-88D at Des Moines, Iowa (not shown), both detected stronger low-level winds than indicated by the Eta analysis.

A better approach to forecasting low-level SR wind speed will come through layer averaging of SR wind speeds using higher-resolution model output (such as in the April 1996 release of PCGRIDDS). Other improvements can result from more accurate storm motion estimates.

7. Operational forecast applications

Based on diagnostic and forecast results from late 1994 through summer 1996, the Eta Model SR wind speed forecast scheme exhibits skill in identifying and forecasting large-scale environments that favor supercell tornadoes. Important aspects of the forecasts are consistency in the forecast areas from one model run to the next, and trends in the SR wind speed forecast areas. For 85% of the 1995 forecast cases where tornadic storms were observed, areas of sufficient ($>$8 m s^{-1}) SR wind speed overlap for the surface and 500 mb were clearly maintained from the 24- to 12-h forecasts. No major systematic problems were noted in forecasts of the SR wind speeds, though forecast error statistics suggest a slight tendency for this technique and the Eta Model to underforecast 500-mb SR wind speed for the

tornadic cases and surface-level SR wind speed for the nontornadic cases, while there is a slight tendency to overforecast surface-level SR wind speed for the tornadic storms. The forecaster should be especially aware of supercell tornado potential when 500-mb SR wind speed is forecast to be sufficient (>8 m s^{-1}), and storm inflow can be enhanced by mesoscale processes (outflow boundaries, mesolows, etc.).

Though SR wind speed forecasts enable reliable forecasts of supercell tornado potential, several other important factors must be considered when utilizing the PCGRIDDS output.

1) Assess the validity of the model forecast *prior* to any detailed analysis of forecast data.
2) Assess the potential for supercell thunderstorms, without which the present SR wind speed technique is irrelevant.
3) Examine the spatial relationships of the various parameters, especially the surface-level and 500-mb SR wind speeds. Cases were documented where the regions of 8 m s^{-1} or greater surface and 500-mb SR wind speeds were not forecast to be in phase (overlapping), but the two regions satifisfying the wind speed criterion were in close proximity. Be wary of the scenario where a well-defined area of sufficient surface SR wind speed is positioned adjacent to a region of sufficient 500-mb SR wind speed, and an axis of large CAPE is located between the favorable SR wind speed areas. Minor inaccuracies in the model forecast, always a concern on the mesoscale, can mask favorable parameter juxtaposition.
4) Consider the temporal evolution of the SR wind speed areas. Several events were documented where the SR wind speeds were not forecast to be in phase at the beginning of a supercell tornado episode, but juxtapositioning of parameters increased with time.
5) Verify the storm motion estimate when examining numerical model output. Once a storm develops, a simple check of storm motions from radar data can quickly alert a forecaster when SR wind speeds may vary substantially from an Eta Model PCGRIDDS forecast.
6) Verify model CAPE forecasts by any available means. Areas forecast to have favorable SR wind speeds, but not supercells, may change.
7) Always remember that other processes contribute to supercell tornadogenesis. The PCGRIDDS analyses can account only for processes resolved by the Eta Model, and the proposed ''thresholds'' of SR wind speed in the PCGRIDDS output are not infallible magic numbers.

Consideration of *forecast and observed* storm-relative shear profiles could also lend confidence or encourage scrutiny in the tornado warning process, especially for warnings based primarily on WSR-88D imagery and algorithm output. It is suspected that the SR wind speed forecasts could help forecasters determine whether or not supercell tornadoes are a major threat with a given scenario. However, it is unclear that the SR conceptual model can enable a forecaster to distinguish between a particular tornadic or nontornadic supercell in warning operations. The SR conceptual model and forecasts may best help forecasters distinguish between situations when supercell tornadoes are more likely and tornado warnings should be considered seriously for any supercells that develop, or when supercells are more likely to be nontornadic and severe thunderstorm warnings *may* be more appropriate.

8. Conclusions

A conceptual model for sustained low-level mesocyclones with tornadic supercells (after Davies-Jones and Brooks 1993, BDC94, and BDW94) was tested using observations and forecasts with the Eta Model. Supercell motions from radar imagery and Eta initial analyses provided a diagnostic assessment of surface-level, 500-, and 250-mb SR wind speeds with both tornadic and nontornadic supercells. These observations yielded a well-defined lower bound to the 500-mb SR wind speed ($\sim$8 m s^{-1}) with tornadic supercells. Storm-relative wind speeds at the surface and 250 mb were quite similar in the mean between the tornadic and nontornadic supercells. The diagnostic evaluation suggests that 500-mb SR wind speed best discriminates between tornadic and nontornadic supercells, and highlights the intermediate range of 500-mb SR wind speed (roughly 7–10 m s^{-1}) where supercells tend to transition from nontornadic to tornadic with increasing SR wind speeds. BRN shear was also examined in comparison to 500-mb SR wind speed as a discriminator between tornadic and nontornadic supercells. Though 500-mb SR wind speed demonstrated a sharper lower bound for the tornadic supercells in this study, BRN shear magnitudes were substantially larger for the tornadic versus nontornadic supercells. Both forecast 500-mb SR wind speed and BRN shear appear to have value as supercell tornado forecast parameters.

Storm-relative wind speed forecasts from PCGRIDDS analyses of Eta Model data have also shown skill in dilineating areas of supercell tornado potential. The forecast test utilized a lower bound of 8 m s^{-1} of surface and 500-mb SR wind speed, determined through the diagnostic evaluation. Forecast areas using the 8 m s^{-1} lower bounds, applied to 51 of the 1995 supercell cases, captured 85% (24 of 28) of the tornadic supercells, with a false alarm ratio of 35% (13 of 37). The most important single finding is the 8 m s^{-1} lower bound to the 500-mb SR wind speed, which represents a necessary, but not sufficient, condition for tornadic supercells. The observations in this study, as well as the forecast statistics, suggest the conceptual model for tornadic supercells from Davies-Jones and Brooks (1993),

DLD93, BDC94, and BDW94 has application for operational forecasts.

The original PCGRIDDS technique has been modified to calculate layer average SR wind speed with the new version of PCGRIDDS released in April 1996, and informal evaluations suggest the layer average quantities are consistent with (and perhaps superior to) the mandatory-level parameters. The PCGRIDDS ''macro'' used in this study, and updated versions, can be downloaded from the Storm Prediction Center home page on the World Wide Web (http://www.nssl.ou.edu/~spc).

Acknowledgments. The author would like to thank Steve Weiss of the Storm Prediction Center (SPC) for constructing the original PCGRIDDS macro and for constant encouragement during this project. The thorough and conscientious efforts of three anonymous reviewers clarified the manuscript and enhanced the findings of this study. Others of the SPC who aided in data collection and reviewed the manuscript: Steve Corfidi, Roger Edwards, Jeff Evans, John Hart, Paul Janish, Bob Johns, Mike Rehbein, Joe Rogash, Joe Schaefer, and Mike Vescio. Thanks also to Harold Brooks, Erik Rasmussen, and Chuck Doswell (all with NSSL) for their helpful discussions.

REFERENCES

Beebe, R. G., 1958: Tornado proximity soundings. *Bull. Amer. Meteor. Soc.,* **39,** 195–201.

Black, T. L., 1994: The new NMC mesoscale eta model: Description and forecast examples. *Wea. Forecasting,* **9,** 265–278.

Bluestein, H. B., and C. R. Parks, 1983: A synoptic and photographic climatology of low-precipitation severe thunderstorms in the southern plains. *Mon. Wea. Rev.,* **111,** 2034–2046.

Branick, M. L., and C. A. Doswell III, 1992: An observation of the relationship between supercell structure and lightning groundstrike polarity. *Wea. Forecasting,* **7,** 143–149.

Brooks, H. E., C. A. Doswell III, and R. Davies-Jones, 1993: Environmental helicity and the maintenance and evolution of low-level mesocyclones. *The Tornado: Its Structure, Dynamics, Prediction and Hazards, Geophys. Monogr.,* No. 79, Amer. Geophys. Union, 97–104.

——, ——, and R. B. Wilhelmson, 1994a: The role of midtropospheric winds in the evolution and maintenance of low-level mesocyclones. *Mon. Wea. Rev.,* **122,** 126–136.

——, ——, and J. Cooper, 1994b: On the environments of tornadic and nontornadic mesocyclones. *Wea. Forecasting,* **9,** 606–618.

Browning, K. A., 1964: Airflow and precipitation trajectories within severe local storms which travel to the right of the winds. *J. Atmos. Sci.,* **21,** 634–639.

Colquhoun, J. R., and P. A. Riley, 1996: Relationships between tornado intensity and various wind and thermodynamic variables. *Wea. Forecasting,* **11,** 360–371.

Darkow, G. L., 1969: An analysis of over sixty tornado proximity soundings. Preprints, *Sixth Conf. on Severe Local Storms,* Chicago, IL, Amer. Meteor. Soc., 218–221.

——, and M. G. Fowler, 1971: Tornado proximity sounding wind analysis. Preprints, *Seventh Conf. on Severe Local Storms,* Kansas City, MO, Amer. Meteor. Soc., 148–151.

Davies, J. M., 1993: Hourly helicity, instability, and EHI in forecasting supercell tornadoes. Preprints, *17th Conf. on Severe Local Storms,* Saint Louis, MO, Amer. Meteor. Soc., 107–111.

Davies-Jones, R., 1984: Streamwise vorticity: The origin of updraft rotation in supercell storms. *J. Atmos. Sci.,* **41,** 2991–3006.

——, and H. E. Brooks, 1993: Mesocyclogenesis from a theoretical perspective. *The Tornado: Its Structure, Dynamics, Prediction and Hazards, Geophys. Monogr.,* No. 79, Amer. Geophys. Union, 105–114.

——, D. Burgess, and M. Foster, 1990: Test of helicity as a tornado forecast parameter. Preprints, *16th Conf. on Severe Local Storms,* Kananaskis Park, AB, Canada, Amer. Meteor. Soc., 588–592.

Doswell, C. A., III, and D. W. Burgess, 1988: On some issues of United States tornado climatology. *Mon. Wea. Rev.,* **116,** 495–501.

——, and ——, 1993: Tornadoes and tornadic storms: A review of conceptual models. *The Tornado: Its Structure, Dynamics, Prediction and Hazards, Geophys. Monogr.,* No. 79, Amer. Geophys. Union, 161–172.

——, R. Davies-Jones, and D. L. Keller, 1990a: On summary measures of skill in rare event forecasting based on contingency tables. *Wea. Forecasting,* **5,** 576–585.

——, A. R. Moller, and R. Pryzbylinski, 1990b: A unified set of conceptual models for variations on the supercell theme. Preprints, *16th Conf. on Severe Local Storms,* Kananaskis Park, AB, Canada, Amer. Meteor. Soc., 40–45.

Droegemeier, K. K., S. M. Lazarus, and R. Davies-Jones, 1993: The influence of helicity on numerically simulated convective storms. *Mon. Wea. Rev.,* **121,** 2005–2029.

Fawbush, E. J., and R. C. Miller, 1952: A mean sounding representative of the tornadic airmass environment. *Bull. Amer. Meteor. Soc.,* **33,** 303–307.

——, and ——, 1954: The types of airmasses in which North American tornadoes form. *Bull. Amer. Meteor. Soc.,* **35,** 154–165.

——, ——, and L. G. Starrett, 1951: An empirical method of forecasting tornado development. *Bull. Amer. Meteor. Soc.,* **32,** 1–9.

Hart, J. A., and W. D. Korotky, 1991: The SHARP Workstation—v1.50. A Skewt/Hodograph Analysis and Research Program for the IBM and compatible PCS. User's manual. NOAA/NWS Forecast Office, Charleston, WV, 30 pp. [Available from NOAA/NWS, Southern Region Scientific Services Division, 819 Taylor Street, Room 10A23, Fort Worth, TX 76102.]

Jahn, D. E., and K. K. Droegemeier, 1996: Simulation of convective storms in environments with independently varying bulk Richardson number shear and storm-relative helicity. Preprints, *18th Conf. on Severe Local Storms,* San Francisco, CA, Amer. Meteor. Soc., 230–234.

Johns, R. H., and C. A. Doswell III, 1992: Severe local storms forecasting. *Wea. Forecasting,* **7,** 588–612.

——, J. M. Davies, and P. W. Leftwich, 1993: Some wind and instability parameters associated with strong and violent tornadoes, 2. Variations in the combinations of wind and instability parameters. *The Tornado: Its Structure, Dynamics, Prediction and Hazards, Geophys. Monogr.,* No. 79, Amer. Geophys. Union, 583–590.

Kerr, B. W., and G. L. Darkow, 1996: Storm-relative winds and helicity in the tornadic thunderstorm environment. *Wea. Forecasting,* **11,** 489–505

Klemp, J. B., 1987: Dynamics of tornadic thunderstorms. *Annu. Rev. Fluid Mech.,* **19,** 369–402.

——, and R. Rotunno, 1983: A study of the tornadic region within a supercell thunderstorm. *J. Atmos. Sci.,* **40,** 359–377.

Lemon, L. R., 1977: New severe thunderstorm radar identification techniques and warning criteria: A preliminary report. NOAA Tech. Memo. NWS NSSFC-1, 60 pp. [Available from NOAA/NWS, Central Region Scientific Services Division, 601 East 12th Street, Kansas City, MO 64106.]

Lilly, D. K., 1986: The structure, energetics and propagation of rotating convective storms. Part II: Helicity and storm stabilization. *J. Atmos. Sci.,* **43,** 126–140.

Maddox, R. A., 1976: An evaluation of tornado proximity wind and stability data. *Mon. Wea. Rev.,* **104,** 133–142.

Rasmussen, E. N., and J. M. Straka, 1998: Variations in supercell

morphology. Part I: Observations of the role of upper-level storm-relative flow. *Mon. Wea. Rev.*, in press.

——, ——, R. Davies-Jones, C. A. Doswell III, F. H. Carr, M. D. Eilts, and D. R. MacGorman, 1994: Verification of the Origins of Rotation in Tornadoes Experiment: VORTEX. *Bull. Amer. Meteor. Soc.*, **75,** 995–1006.

Rotunno, R., and J. B. Klemp, 1985: On the rotation and propagation of simulated supercell thunderstorms. *J. Atmos. Sci.*, **42,** 271–292.

Stensrud, D. J., J. V. Cortinas Jr., and H. E. Brooks, 1997: Discriminating between tornadic and nontornadic thunderstorms using mesoscale model output. *Wea. Forecasting*, **12,** 613–632.

Wakimoto, R. M., and J. W. Wilson, 1989: Non-supercell tornadoes. *Mon. Wea. Rev.*, **117,** 1113–1140.

Weisman, M. L., 1996: On the use of vertical wind shear versus helicity in interpreting supercell dynamics. Preprints, *18th Conf. on Severe Local Storms*, San Francisco, CA, Amer. Meteor. Soc., 200–204.

——, and J. B. Klemp, 1982: The dependence of numerically simulated convective storms on vertical wind shear and buoyancy. *Mon. Wea. Rev.*, **110,** 504–520.

——, and ——, 1984: The structure and classification of numerically simulated convective storms in directionally varying wind shears. *Mon. Wea. Rev.*, **112,** 2479–2498.

——, and ——, 1986: Characteristics of isolated convective storms. *Mesoscale Meteorology and Forecasting*, P. S. Ray, Ed., Amer. Meteor. Soc., 331–358.

Wicker, L. J., 1996: The role of near surface wind shear on low-level mesocyclone generation and tornadoes. Preprints, *18th Conf. on Severe Local Storms*, San Francisco, CA, Amer. Meteor. Soc., 115–119.

——, and R. B. Wilhelmson, 1995: Simulation and analysis of tornado development and decay within a three-dimensional supercell thunderstorm. *J. Atmos. Sci.*, **52,** 2675–2703.

Zubrick, S. M., and E. Thaler, 1993: Enhancements to the operational forecast process using gridded model data. Preprints, *13th Conf. on Weather Analysis and Forecasting*, Vienna, VA, Amer. Meteor. Soc., 5–9.